JOURNAL OF MECHANICAL ENGINEERING AND SCIENCES
ISSN: 2289-4659 e-ISSN: 2231-8380
VOLUME 17, ISSUE 3, 2023, 9586 – 9596
DOI: https://doi.org/10.15282/jmes.17.3.2023.5.0759

RESEARCH ARTICLE

The analysis of grid independence study in continuous disperse of MQL delivery system

Z. Zulkifli[1], N.H. Abdul Halim[1]*, Z.H. Solihin[1], J. Saedon[1], A.A. Ahmad[1], A.H. Abdullah[1], N. Abdul Raof[2], and M. Abdul Hadi[3]

[1] School of Mechanical Engineering, College of Engineering, Universiti Teknologi MARA, 40450, Shah Alam, Malaysia
[2] Department of Manufacturing and Materials Engineering, Kulliyyah of Engineering, International Islamic University Malaysia, 53100, Gombak, Malaysia
[3] Faculty of Manufacturing and Mechatronic Engineering Technology, College of Engineering Technology, Universiti Malaysia Pahang, 26600, Pekan, Malaysia

ABSTRACT - A sustainable cutting method of Minimum Quantity Lubricant (MQL) was introduced to promote lubrication effect and improve machinability. However, its performances are very dependent on the effectiveness of its mist to penetrate deep into the cutting zone. Optimizing the MQL system requires massive experimental work that increases cost and time. Therefore, this study conducts Computational Fluid Dynamic (CFD) analysis using ANSYS Fluent and focuses on the grid independence study in dispersed-continuous phase of MQL delivery system. The main aim is to identify the best mesh model that influences the accuracy of the CFD model. The analysis proposed two different unstructured grid cell elements of quadrilateral and triangular that were only applicable for 2-dimensional fluid flow in CFD. The unstructured grid was controlled with three different mesh quality factors such as Relevance Center, Smoothing, and Span Angle Center at coarse /low, medium, and fine /high. The results showed that the best mesh quality for quadrilateral was at 60,000 nodes number and coarse mesh, whereas the triangular was at 90,000 nodes number and coarse mesh. Both combinations resulted the most consistent and reliable result when compared with past studies. However, this study decided to choose quadrilateral cell element with 60,000 nodes number and coarse mesh as it is considered to be sufficient to provide accurate and reliable result as well as practical in terms of computational time for the MQL model in CFD analysis.

ARTICLE HISTORY
Received : 04th Apr. 2023
Revised : 15th June 2023
Accepted : 15th July 2023
Published : 28th Sept. 2023

KEYWORDS
MQL
Sustainable
Grid independence
Mesh analysis
CFD

1.0 INTRODUCTION

Inconel 718 is known as a difficult-to-cut material due to its superior mechanical and chemical properties such as high heat resistant, oxidation, and tensile strength. Consequently, its strength has led to low thermal conductivity and tendency of work hardening particularly at high temperature. This happens when cutting heat is produced rapidly at high cutting speed and poorly dissipated due to its low thermal conductivity which resulted in material hardening. At the same time, the accumulated heat is transferred to cutting tool that decreases the tool life [1]. Therefore, a sustainable Minimum Quantity Lubricant (MQL), which is a semi-dry machining, has been introduced that offers effective cooling-lubrication effect with minimal amount of cutting fluid under high air pressure that is supplied in a mist form directly into the cutting zone [2]. However, the performances of MQL machining are very dependent on the effectiveness of its mist to penetrate and provide lubrication effect deep into the cutting zone [3]. For instance, Zhu et al. [4] studied the effect of MQL spray, droplet transportation and penetration with varying spindle rotation, air flow rate, and nozzle distance. They found that nozzle distance has the most dominant influence on the cutting force and surface roughness in the milling process. Meanwhile, Liu et al. [5] investigated the effect of cutting force and temperature of milling titanium alloy with different MQL parameters such as air pressure, oil flow rate, and nozzle angle. The results showed that the penetration ability is mostly influenced by the oil flow rate for penetration performance that corresponds to the measure respond.

Considering the challenge to develop an effective dispersed-continuous phase of MQL system requires high cost and time consuming especially in large scale of repetition experimental works. Thus, simulation work has emerged as an alternative method to perform investigation to establish a proper model for the selected MQL parameters. Literature studies show that the Computational Fluid Dynamics (CFD) is one of the common computational approaches used as it offers effective analysis of fluid flow and heat transfer which replace massive experimental studies [6–8]. In other studies of MQL approach, CFD was utilized by Awale et al. [9], and Zan et al. [10] to analyse the influence of different MQL properties on the mist flow lubrication effect. As reported, CFD was found efficient for fluid flow analysis as it is capable to analyse the flow behaviour and visualize the penetration performance of the continuous disperse of MQL mist during machining. Generally, during machining, cutting fluid is dispersed continuously by pressurized air to form the MQL mist flow.

***CORRESPONDING AUTHOR | N. H. Abdul Halim|** ✉ hayatihalim@uitm.edu.my

In CFD analysis, it is essential to establish a quality model where mesh independence plays an important part for model development, validation, and verification. The aim of mesh independence analysis is to identify the optimal mesh model that will influence the accuracy of the CFD model. For instance, Xu et al. [11] found that the coarse mesh type is the best as compared to medium and fine types in satisfying the accuracy needs. This is parallel to Knotek et al. [12] as they found that the coarse mesh is sufficient with advantages in terms of cost and time consuming to conduct the CFD analysis. However, contradict result was reported by Nordin et al. [12] where fine mesh was selected as the optimum model between meshes order in their flow behavior study. According to them, the fine mesh generated more accurate output of aerodynamic coefficient with presentable fluid flow image. Meanwhile, Iranzo et al. [13] informed that the increase of element numbers has resulted in more accurate or closer to the real result that was performed physically in experimental work. Previous literatures also showed that other mesh quality factors such as aspect ratio [13], skew angle [14] or mesh deformation must be considered in mesh independence study.

In order to meet the accuracy of the model, different mesh quality parameters in mesh independence study can be performed. For instance by using Proton Exchange Membrane Fuel Cell (PEMFC) module that was used for mesh independence study with the mesh quality parameter aspect ratio by using Best Practice Guidelines [13], or by using surface skewness [14] to investigate the effects on biofilm development. Thus, in this study, mesh independence is developed by using ANSYS Fluent V16 technology of Computational Fluid Dynamics (CFD) where the simulation works were performed with three different mesh types of course, medium, and fine, for both quadrilateral and triangular cell element types. Other ANSYS parameters with respect to flow velocity and flow behaviour were also established to identify the best types of mesh to suit with the current MQL delivery system model for the dispersed-continuous phase study.

2.0 MATHEMATICAL MODELLINGS

In this paper, a 2D-symmetrical MQL delivery model was established as shown in Figure 1 by referring to Najiha et al. [15], Pereira et al. [16], and Subramani et al. [17] as the main references to develop the concept. For mesh independence study, two types of unstructured grids which are quadrilateral and triangular were applied at three different mesh orders: coarse/low, medium, and fine/high. The model was simulated using Computational Fluid Dynamics (CFD) codes in ANSYS Fluent software where the results of velocity was compared with the results reported by Najiha et al. [15], Pereira et al. [16], and Subramani et al. [17]. The main aim is to evaluate and identify the best types of cell elements and meshes order for the dispersed-continuous phase of MQL delivery system as accuracy and performance are the main goals in thorough CFD simulation [11]. The CFD approach was selected as it gives better fluid flow images than experimental work in terms of mist flow properties and behaviour. All the important inputs such as nozzle design and geometry as well as material properties were particularly referred to Najiha et al. [15]. This is because, they provide reliable and complete information in terms parameters and results that significant to be referred for the validation and comparison analysis. Other than that, their MQL model system is also nearly similar to the MQL model system in this study.

Figure 1. The schematic free body diagram of MQL model and boundary conditions in CFD

The continuity Eq. (1) and momentum Eq. (2) of Navier-Stokes are derived to determine the input and output parameters of the fluid flow that are also defined as the boundary conditions.

Continuity equation:

$$\frac{\partial \rho}{\partial t} + \vec{\nabla} \cdot \vec{V} = 0 \tag{1}$$

Momentum equation:

$$\rho \frac{\partial \vec{V}}{\partial t} + \rho(\vec{V} \cdot \vec{\nabla})\vec{V} = \overrightarrow{\rho g} - \vec{\nabla} P + \mu \nabla^2 V \tag{2}$$

where V is the flow velocity vector, ρ is the density, P is the pressure, and g is the acceleration of gravity.

The governing equations for steady state, incompressible, adiabatic, and frictionless two-phase flow are solved during simulation throughout the domain. The velocity is computed horizontally as the fluid flows in x-direction where the continuity equation in Eq. (1) is then derived into Eq. (3).

$$\frac{\partial u}{\partial x} = 0 \tag{3}$$

The expansion of momentum equation in Eq. (2) is shown in Eq. (4).

$$\rho\left(\frac{\partial u}{\partial t} + u\frac{\partial u}{\partial x} + v\frac{\partial u}{\partial y} + w\frac{\partial v}{\partial z}\right) = -\frac{\partial P}{\partial x} + \rho g_x + \mu\left(\frac{\partial^2 u}{\partial x^2} + \frac{\partial^2 u}{\partial y^2} + \frac{\partial^2 v}{\partial z^2}\right) \tag{4}$$

where u and v are the velocity components in longitudinal and vertical coordinates, respectively, while w is the vertical coordinate; and μ is the viscosity. The momentum equation in Eq. (4) is then simplified into Eq. (5).

$$udu + vdv + \frac{\partial P}{\rho} = 0 \tag{5}$$

Eq. (5) is then mathematically integrated in Eq. (6) to define the flow boundary conditions. Then, Eq. (7) is derived as an outcome from the integration of Eq. (6).

$$\int_a^b u\, du + \int_a^b v\, dv + \int_a^b \frac{\partial p}{\rho} = 0 \tag{6}$$

$$\frac{1}{2}(u_b^2 - u_a^2) + \frac{1}{2}(v_b^2 - v_a^2) + \frac{1}{\rho}(P_{2-}P_1) = 0 \tag{7}$$

Eq. (7) is then rearranged with the summation of input 1 for oil lubricant and input 2 for air that are equal to the output which is a continuous-dispersed of two-phase flow. Then, unknown output parameters are identified which include the density, ρ_3, and output velocity, V_3, that make it difficult to solve the equation. Thus, the mass flow rate, $\dot{m}$ summation as in Eq. (8) is substituted with the unknown output parameters as the mass flow rate is equal to the multiplication of the density, ρ, velocity, V and area, A. Then, the output density, ρ_3 is substituted into Eq. (7), which is then expanded in Eq. (9). The derivation and rearrangement of Eq. (9) resulted into Eq. 10, where it proposes the output velocity, V_3 as the output for this fluid flow study.

$$\dot{m}_1 + \dot{m}_2 = \dot{m}_3 \tag{8}$$

$$\left(\Delta P_1 + \frac{\rho_1 \Delta {V_1}^2}{2}\right) + \left(\Delta P_2 + \frac{\rho_2 \Delta {V_2}^2}{2}\right) = \left[2\Delta P_3 + \left(\frac{\rho_1 V_1 A_1 + \rho_2 V_2 A_2}{V_3 A_3}\right)\Delta {V_3}^2\right] \tag{9}$$

$$V_3 = \frac{\left(2\Delta P_1 A_3 + \rho_1 \Delta {V_1}^2 A_3\right) + \left(2\Delta P_2 A_3 + \rho_2 \Delta {V_2}^2 A_3\right) - \left(2\Delta P_3 A_3\right)}{\left(\rho_1 V_1 A_1 + \rho_2 V_2 A_2\right)} \tag{10}$$

where V_3 is the output parameter that is being governed by the influence of, V_1, V_2, P_1, P_2, ρ_1, and ρ_2 as the input factors and details as per discussed in Table 1. As for the areas of A_1, A_2, and A_3, and P_3, they are treated as constant parameters.

2.1 Governing Equations and Modelling

For simulation, the parameters used for the boundary conditions were referred to Najiha et al. [15] as listed in Table 1. The simulation conducted in ANSYS Fluent was governed by the continuity and momentum equations which were used in two-phase steady flow. The multiphase model selected was the Volume of Fluid (VOF) model where two-phase flows were utilized for the air pressure and oil lubricant. According to Mousavi et al. [18], the VOF model is suggested as it is suitable for free-surface flow simulation. Therefore, the phase volume fraction as in Eq. (11) is introduced in order to capture the interface between two phases of air and oil lubricant.

Table 1. Parameters for simulation model analysis

Parameters	Values/Conditions
Geometry	2-dimensional
Models	Multiphase: Volume of Fluid (VOF) Turbulence: Standard k-epsilon
Solver	Pressure-based, steady state
Solution method	SIMPLE pressure coupling scheme
Initialization	Hybrid

Table 1. (cont.)

Parameters	Values/Conditions
Nozzle air inlet diameter (mm)	2
Nozzle oil inlet diameter (mm)	2
Nozzle outlet diameter (mm)	2
Air density, ρ_1 (kg/m^3)	1.225
Air viscosity (kg/m^{-s})	1.7894x10^{-5}
Air flowrate (l/hr)	72.6
Oil density, ρ_2 (kg/m^3)	960
Oil viscosity (kg/m^{-s})	88x10^{-4}
Oil flowrate (ml/min)	15
Air inlet velocity, V_1 (m/s)	231
Air inlet pressure, P_1 (kPa)	400
Oil inlet velocity, V_2 (m/s)	0.00133
Oil inlet pressure, P_2 (kPa)	0
Outlet pressure, P_3 (kPa)	0

In VOF multiphase computational, the sum of all phases is equivalent to unity where the less density (gas phase) which is air is designated as the primary phase, while the denser density (liquid phase) which is oil lubricant is designated as the secondary phase [19].

$$\alpha_{air} + \alpha_{oil} = 1 \tag{11}$$

where, α_{air} and α_{oil} are the volume fractions of the air phase and oil lubricant phase, respectively.

In this study, the model is in turbulent flow based on the Reynolds number calculation. Thus, standard k-ε model is selected as it is fit and suitable to study the centre flow of the MQL mist flow throughout the domain. The model is also known as stable and accurate turbulence in terms of fluid flow and heat transfer studies for simulation [20]. This turbulence model consists of two equations which are turbulent kinetic energy, *k*, as in Eq. (12) and turbulent energy dissipation, ε, as in Eq. (13).

$$\nabla \cdot \left(\rho \vec{V}\, k\right) = \nabla \cdot \left[\left(\mu + \frac{\mu_t}{\sigma_k}\right) \nabla k\right] + P_k - \rho\varepsilon \tag{12}$$

$$\nabla \cdot \left(\rho \vec{V}\, \varepsilon\right) = \nabla \cdot \left[\left(\mu + \frac{\mu_t}{\sigma_\varepsilon}\right) \nabla \varepsilon\right] + \frac{\varepsilon}{k} C_{1\varepsilon} P_k - \frac{\varepsilon^2}{k} C_{2\varepsilon} \rho \tag{13}$$

where μ is the laminar viscosity. The turbulent viscosity model, μ_t is presented in Eq. (14), and the other related constant parameters information are shown in Table 2.

$$\mu_t = C_\mu \rho \frac{k^2}{\varepsilon} \tag{14}$$

For the solution method, Semi-Implicit Method for Pressure-Linked Equation (SIMPLE) algorithm type is used for the Pressure-Velocity Coupling Method to solve the scalar variables and to simulate the spray behaviour.

Table 2. Constant parameters information of k-**ε** turbulent model

Parameters	Value
$C_{1\varepsilon}$	1.44
$C_{2\varepsilon}$	1.92
C_μ	0.09
σ_k	1.0
σ_ε	1.3

2.2 Meshing

In this study, meshing control operations of Global Meshing Controls were performed to identify the influence of mesh analysis towards the accuracy and performance of CFD simulation by ANSYS Fluent. Cell element types of quadrilateral and triangular were generated for the meshing analysis. Then, 2D-symmetrical MQL models with quadrilateral and triangular element types were controlled by four different meshing factors: Relevance Center, Smoothing, Span Angle Center, and Curvature Normal Angle, as shown in Table 3. In ANSYS environment, the function

of Relevance Center is to set a specific mid-point value of the Relevance by the slider control. Meanwhile, the Smoothing is the intention to improve the element quality by moving the nodes. For the Span Angle Center, it is one of the normal angles setting under Curvature that indicates the maximum allowable angle for one element edges to be allowed to span. All these parameters are set to coarse/low, medium, and fine/high, separately for each element type. For the Curvature, it is used to control basic mesh sizing of advanced size functions. It checks curvature on edges and faces and sets element sizes in order to avoid them exceeding the maximum size or the curvature angle. To perform the meshing analysis with all the parameters, both types of cell element, quadrilateral and triangular, were simulated at five different number of nodes which were 5,000, 15,000, 30,000, 60,000, and 90,000.

Table 3. Controlled factors of meshing operations

Unstructured Grid	Relevance Center	Smoothing	Span Angle Center	Curvature Normal Angle (°)
Quadrilateral /Triangular	Coarse	Low	Fine	90
	Medium	Medium	Medium	75
	Fine	High	Fine	36

3.0 RESULTS AND DISCUSSION

3.1 Comparison between Quadrilateral and Triangular Cell Element at Different Nodes Number

Results of flow velocity for coarse, medium, and fine mesh types at different nodes number using quadrilateral and triangular cell elements were compared as shown in Figure 2 and Figure 3, respectively. The velocity values were taken at distances of 3.75 mm, 7.5 mm, and 11.25 mm to clearly show the flow progress with respect to flow distances. For quadrilateral cell elements as in Figure 2, it shows that the gap of flow velocity between meshes type was getting smaller for similar flow pattern with the increase of nodes numbers. However, nodes number of 30,000 to 90,000 resulted with more accurate results where the velocity flow of each mesh type was evidently similar. This finding in parallel with Iranzo et al. [13] who reported that their best results were generated at the highest nodes and elements number. Also, it can be seen from Figure 2 that the velocity flows at 60,000 to 90,000 nodes numbers decreased gradually with flow distance. This phenomenon is considered as normal for MQL mist flow as it decreases with the distance [21]. They also resulted with similar flow pattern at different meshes type.

The vertical bar graph in Figure 4 represents the flow velocity of each node number for better justification. Clearly, it can be said that quadrilateral cell elements with nodes number of 60,000 to 90,000 resulted with more accurate, consistent, and stable velocity flow for the MQL model in CFD analysis. Nevertheless, 60,000 nodes number is preferred in this study since the computer memory or computation time is also the determining factor. Luis et al. [22] also applied lower element numbers to optimize the both CFD model accuracy and computational effort. However, Chowdhury et al. [23] preferred to use highest elements number in their study to achieve the acceptable result though they had mentioned that it was impractical as it takes a lot of computational time. Meanwhile, for the triangular cell elements as shown in Figure 3, it was found that the flow velocity of each mesh type with 30,000 to 90,000 nodes number gradually decreased with similar and stable flows pattern. However, when referring to the vertical bar graph in Figure 5, it can be said that only at 90,000 nodes number resulted with accurate and stable velocity flow for the MQL model. Thus, it can be decided that the highest nodes number at 90,000 is the best mesh quality for triangular cell element. When compared with Wu et al. [24] who also applied triangular cell element at two different nodes and elements number, they decided to choose the lower values as it is sufficient to generate accurate result that is closer to larger nodes and elements number. As suggested by Chowdhury et al. [23], appropriate nodes and elements number are important for the CFD model accuracy and simulation run time. Thus, this emphasizes that highest nodes number is not necessarily important as long as the objectives of the study in terms of CFD model accuracy and less computational time are achieved.

For MQL machining, the CFD model accuracy is important particularly for MQL mist flow analysis of high-speed cutting in order to ensure the lubrication effect flows sharply deep into the contact point between the cutting tool edge and workpiece interface. As reported by López De Lacalle et al. [25], MQL was found to be very effective in lubrication effect once it entered the backflow milling after optimizing it in CFD environment. Similarly, Rahim et al. (2015) managed to optimize the MQL mist flow by analyzing the influence of various MQL parameters through simulation works of CFD as shown in Figure 6. As the tool wear rate and machined surface quality critically depend on cutting temperature that relies on the MQL performance, detail analysis is significantly required for better machinability.

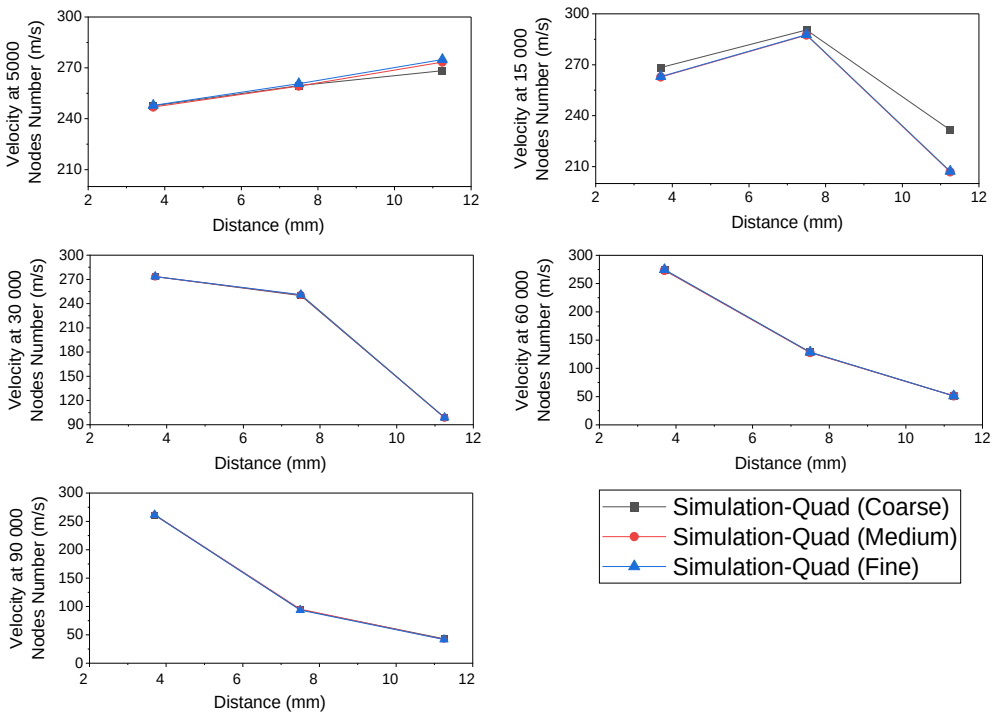

Figure 2. Flow velocity at different nodes number of 5,000, 15,000, 30,000, 60,000, and 90,000 for coarse, medium, and fine mesh types in quadrilateral

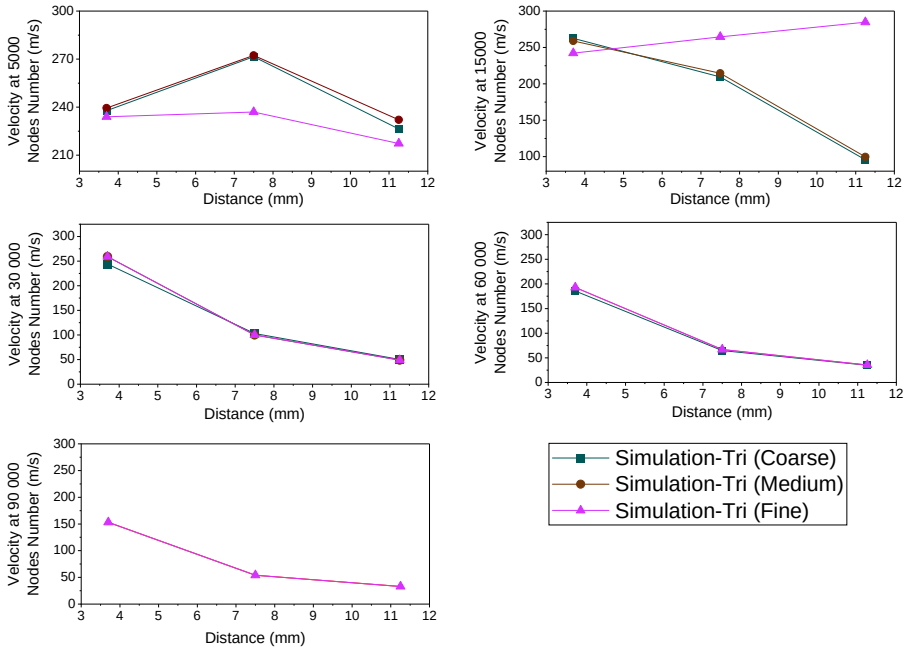

Figure 3. Flow velocity at different nodes number of 5,000, 15,000, 30 000, 60,000, and 90,000 for coarse, medium, and fine mesh types in triangular cell element

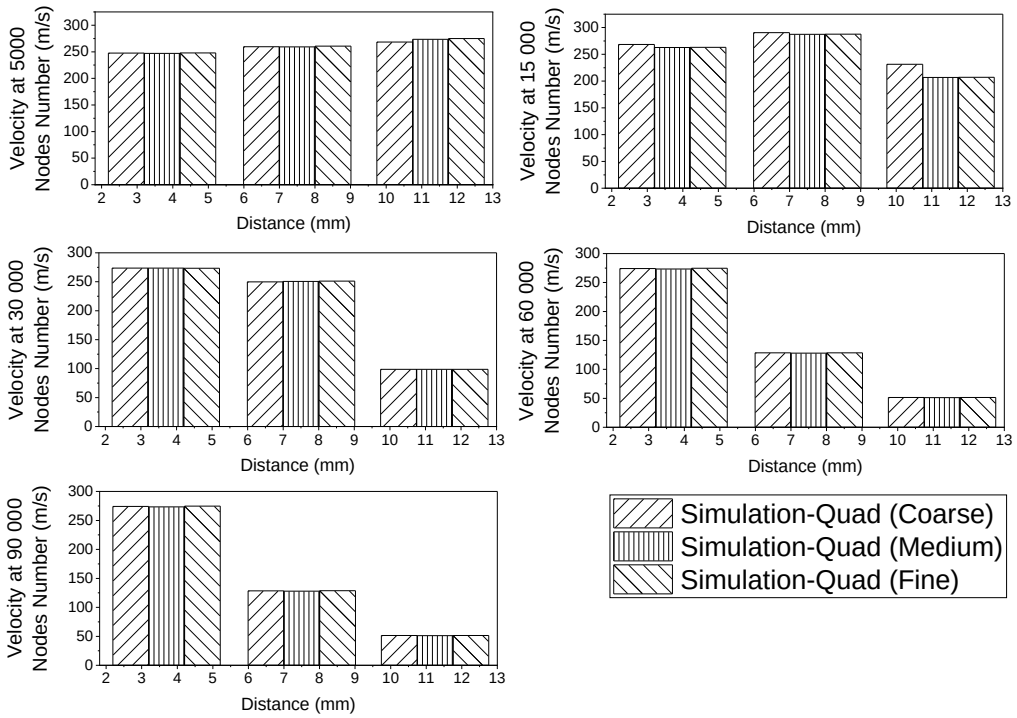

Figure 4. Comparison of flow velocity using quadrilateral cell elements at 5,000 to 90,000 nodes number for coarse, medium, and fine meshes types

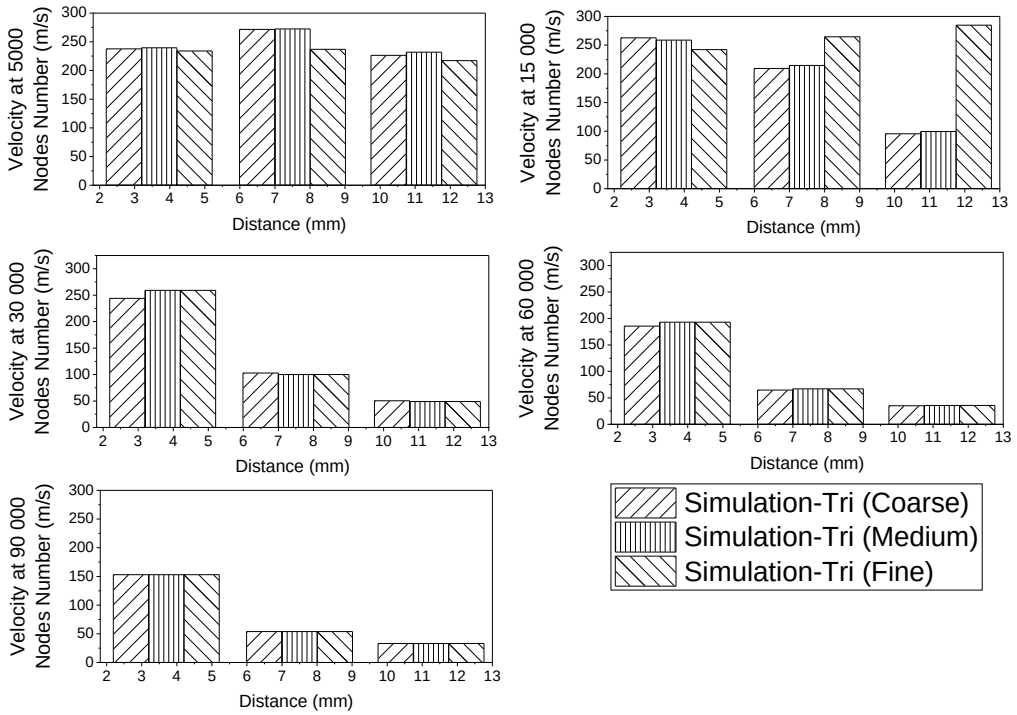

Figure 5. Comparison of flow velocity using triangular cell elements at 5,000 to 90,000 nodes number for coarse, medium, and fine meshes types

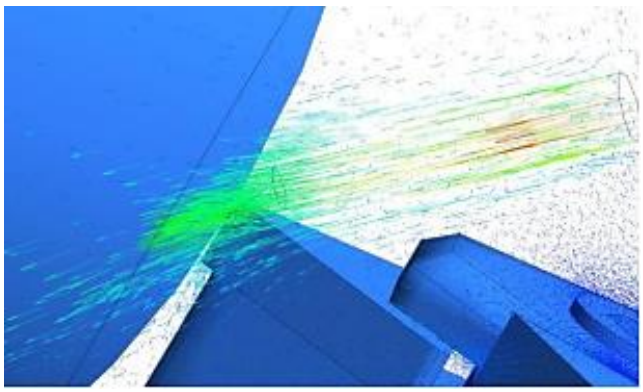

Figure 6. Model geometry by [26] in CFD analysis of the influence of flow pattern with nozzle distances and input pressure

Figures 7 and 8 illustrate the MQL mist flow model in CFD environment at different node numbers when they entered the domain and passed through the quadrilateral and triangular cell elements, respectively. These CFD flow diagrams are essential for presenting well and clear visual resolution of continuous dispersed flow for better understanding of mesh quality as well as to develop detailed analysis. It is also important for CFD analysis to set the right iteration number as it is a step to generate a complete computational study and accurate result [24, 27]. For instance, Growth et al. [28] simulated their CFD MQL mist flow at different iterations number to properly match the distributions of the particles. While Figures 7 and 8 show that at 40 iterations, the flow lengths were shortened with the increase of node number. Thus, this clearly demonstrates that larger iteration number is required for larger number of nodes in order to generate a complete MQL mist flow image during CFD simulation. Figure 9 shows that a complete MQL mist flow pattern at 60,000 nodes can only be generated at 120 iterations, where its computational time was almost 50% longer as compared to 40 iterations. This was also mentioned by Ahmad et al. [29] as they compared a CFD model of base size at 100 mm and 50 mm which found that the smaller mesh base sizes required 4 times more simulation run time. However, they also emphasized that the smaller cells size provided better resolution as implied in their study that the smaller cells used around the car geometry model provided high resolution of the wake region behind the car. This phenomena in CFD was also supported by Falcone et al. [30], which highlighted that the implication of inadequate mesh quality resulted in poor resolution. Therefore, this effort is compulsory for an accurate and reliable simulation results.

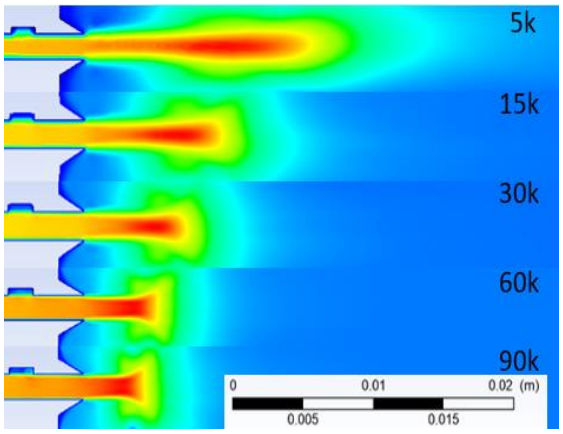

Figure 7. MQL mist flow pattern using quadrilateral cell elements at 40 iterations

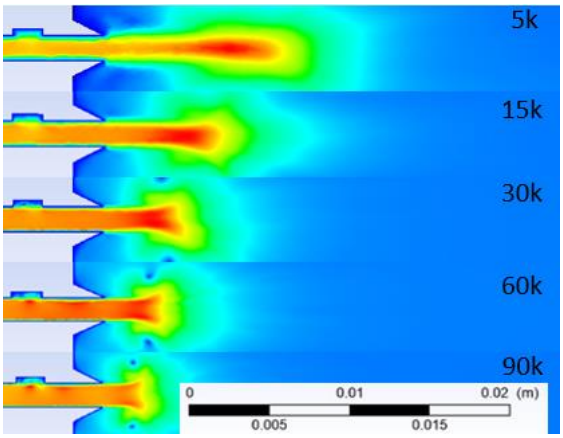

Figure 8. MQL mist flow pattern using triangular cell elements at 40 iterations

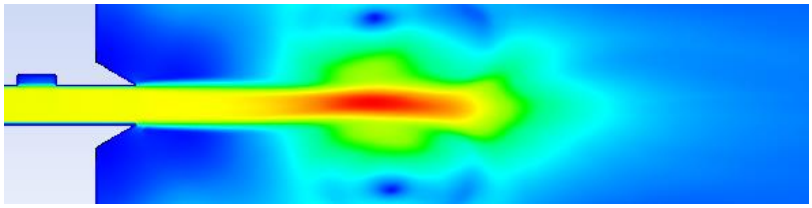

Figure 9. MQL mist flow pattern using quadrilateral cell element at 60,000 nodes number and 120 iterations

3.2 Comparison between Quadrilateral and Triangular Cell Element at Different Meshes Type

For further analyses, each flow velocity pattern with coarse, medium and fine mesh types using quadrilateral and triangular cell elements, both with 60,000 and 90,000 nodes number, was compared with Najiha et al. [15], as shown in Figure 10 and Figure 11, respectively. As shown in Figure 11, the analysis for the flow velocity using 90,000 nodes number developed the most stable MQL mist flow model as each meshes type of both quadrilateral and triangular cell elements had similar and close pattern to each other. For the velocity flow using 60,000 nodes number as in Figure 10, it shows a slightly different pattern between mesh types for triangular cell element, but obviously similar pattern using the quadrilateral. At the same time, the quadrilateral cell elements also resulted closer velocity flow values and patterns with Najiha et al. [15], as compared to triangular. In order to select the right combination that will result with accurate analysis yet shorter computational time, CFD analysis with coarse mesh type and 60,000 nodes number of quadrilateral cell element is more preferred to be used in this study. In parallel, Xu et al. [11] also performed the mesh analysis with three different meshes of course, medium, and fine which resulted coarse mesh as the optimal choice to generate the lowest computational cost simulation. This approach was also implemented by Chowdhury et al. [23] where they used coarse mesh in order to generate better quality mesh with less time consumption of simulation.

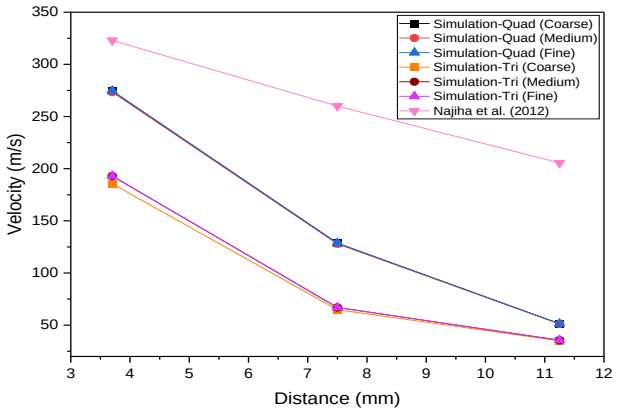

Figure 10. Flow velocity of different meshes type using quadrilateral and triangular cell element at 60,000 nodes number

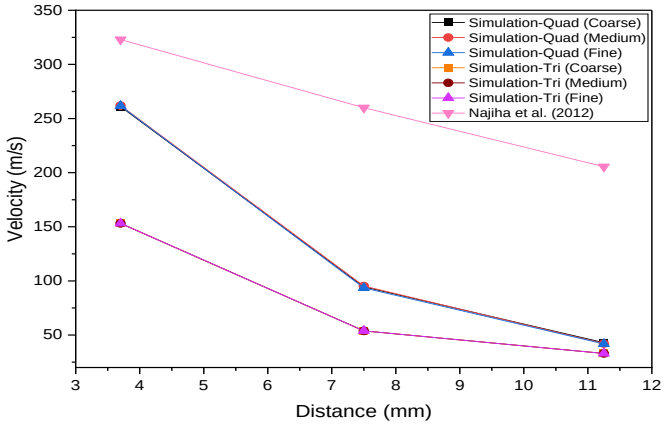

Figure 11. Flow velocity of different meshes type using quadrilateral and triangular cell element at 90,000 nodes number

3.3 Validation with Previous Studies

By using coarse mesh type with 60,000 nodes number of quadrilateral element, the velocity flow pattern of MQL mist flow was compared with literatures of Najiha et al. [15], Pereira et al. [16], and Subramani et al. [17] as depicted in Figure 12. The simulation results show that the velocity flow pattern is very similar with Najiha et al. [15] and Pereira et al. [16], but contradicts with Subramani et al. [17]. This is because Subramani et al. [17] applied different MQL parameters and incomplete information were shared in their study. Meanwhile, the highest velocity generated by Pereira et al. [16] was probably due to the application of high oil flow rate and air pressure with smaller outlet nozzle diameter. This is in line with Jadhav and Deivanathan et al. [31] who reported that the increase of air pressure and oil flow rate increases the flow velocity of MQL flow behaviour in the study of CFD.

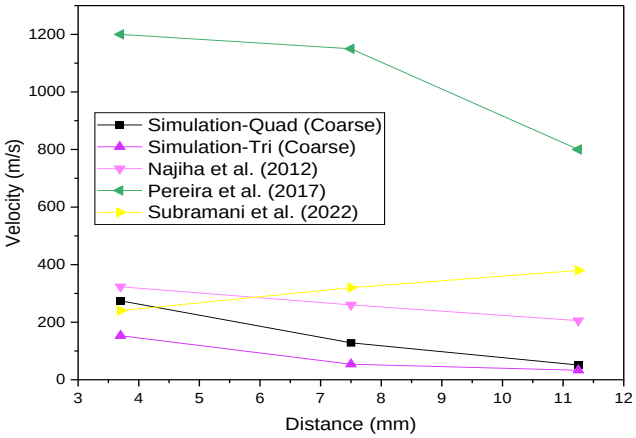

Figure 12. Comparison of velocity between quadrilateral and triangular with previous studies

4.0 CONCLUSIONS

In this study, a simulation technique by ANSYS Fluent was used to perform a mesh analysis for grid independence to identify the most appropriate yet feasible CFD model. This study proposed the result of the output flow velocity as it is an important parameter in fluid flow study for two different cell element types of quadrilateral and triangular with the setting of mesh quality factors of Relevance Center, Smoothing, Span Angle Center, and Curvature Normal Angle that are set as coarse/low, medium, and fine/high for each factor. The findings showed that the best MQL model for quadrilateral was at 60,000 nodes number with coarse mesh type, while triangular best MQL model was at 90,000 nodes number with coarse mesh type. Thus, the study of mesh quality analysis showed that the selected model can provide an accurate and reliable result with time and cost saving in order to develop dispersed-continuous phase of MQL delivery system by CFD.

5.0 ACKNOWLEDGMENTS

Acknowledgment is given to the Government of Malaysia, and Universiti Teknologi MARA for providing the research fund (Grant No.: 600-RMC/SRC/5/3 (029/2020).

6.0 REFERENCES

[1] N. H. Abdul Halim, C. H. Che Haron, J. Abdul Ghani, and M. F. Azhar, "Response Surface Methodology (RSM) based analysis for tool life optimization in cryogenic CO_2 milling of Inconel 718," *IOP Conference Series: Materials Science and. Engineering*, vol. 606, no. 1, pp. 1 - 10, 2019.

[2] G. Zhu, S. Yuan, X. Kong, C. Zhang, and B. Chen, "Experimental observation of oil mist penetration ability in minimum quantity lubrication (MQL) spray," *Journal of Mechanical Science and Technology*, vol. 34, no. 8, pp. 3217–3225, 2020.

[3] K. L. J. Kiat, N. I. K. Ismail, N. Rosli, and E. A. Alias, "Study of nozzle distance and oil flow rate effects on the droplets size of minimum quantity lubrication," *IOP Conference Series: Materials Science and Engineering*, vol. 1062, no. 1, 2021.

[4] G. Zhu, S. Yuan, and B. Chen, "Numerical and experimental optimizations of nozzle distance in minimum quantity lubrication (MQL) milling process," *International Journal of Advanced Manufacturing Technology*, vol. 101, no. 1–4, pp. 565–578, 2019.

[5] Z. Q. Liu, X. J. Cai, M. Chen, and Q. L. An, "Investigation of cutting force and temperature of end-milling Ti-6Al-4V with different minimum quantity lubrication (MQL) parameters," in *Proceedings of the Institution of Mechanical Engineers, Part B: Journal of Engineering Manufacture*, vol. 225, no. 8, pp. 1273–1279, 2011.

[6] W. El-Bouri, I. Deiab, K. Khanafer, and E. Wahba, "Numerical and experimental analysis of turbulent flow and heat transfer of minimum quantity lubrication in a turning process using discrete phase model," *International Communications in Heat Mass Transfer*, vol. 104, pp. 23–32, 2019.

[7] K. Khanafer, I. Deiab, and W. El-Bouri, "Numerical analysis of flow and heat transfer of minimum quantity lubrication in a turning process using inconel alloy," *The International Journal of Advanced Manufacturing Technology*, vol. 108, pp. 475–483, 2020.

[8] Y. You, S. Wang, W. Lv, Y. Chen, and U. Gross, "A CFD model of frost formation based on dynamic meshes technique via secondary development of ANSYS fluent," *International Journal of Heat and Fluid Flow*, vol. 89, p. 108807, 2021.

[9] A. S. Awale, M. Vashista, and M. Z. Khan Yusufzai, "Multi-objective optimization of MQL mist parameters for eco-friendly grinding," *Journal of Manufacturing Processes*, vol. 56, pp. 75–86, 2020.

[10] Z. Zan, K. Guo, J. Sun, X. Wei, Y. Tan, and B. Yang, "Investigation of MQL parameters in milling of titanium alloy," *The International Journal of Advanced Manufacturing Technology*, vol. 116, no. 1–2, pp. 375–388, 2021.

[11] X. Xu, H. Li, and Y. Lin, "Mesh-order independence in CFD simulation," *IEEE Access*, vol. 7, p. 119069–119081, 2019.

[12] S. Knotek, S. Schmelter, and M. Olbrich, "Assessment of different parameters used in mesh independence studies in two-phase slug flow simulations," *Measurement: Sensors*, vol. 18, pp. 3–6, 2021.

[13] A. Iranzo, B. Toharias, C. Suárez, F. Rosa, and J. Pino, "Dataset and mesh of the CFD numerical model for the modelling and simulation of a PEM fuel cell," *Data in Brief*, vol. 41, p. 107987, 2022.

[14] P. M. Roveto, A. Gupta, and A. J. Schuler, "Effects of surface skewness on local shear stresses, biofilm activity, and microbial communities for wastewater treatment," *Bioresouce Technology*, vol. 320, p. 124251, 2021.

[15] A. R. Y. and K. K. M. S. Najiha, M. M. Rahman, M. Kamal, "Minimum quantity lubricant flow analysis in end milling process: A computational fluid dynamics approach," *Journal of Mechanical Engineering and Sciences*, vol. 3, pp. 340–345, 2012.

[16] O. Pereira, A. Rodríguez, J. Barreiro, A. I. Fernández-Abia, and L. N. L. de Lacalle, "Nozzle design for combined use of MQL and cryogenic gas in machining," *International Journal of Precision Engineering and Manufacturing - Green Technology*, vol. 4, no. 1, pp. 87–95, 2017.

[17] S. Subramani, S. Nantha Muthu, and N. L. Gajbhiye, "A numerical study on the influence of minimum quantity lubrication parameters on spray characteristics of rapeseed oil as cutting fluid," *Industrial Lubrication and Tribology*, vol. 74, no. 2, pp. 197–204, 2022.

[18] S. M. Mousavi, A. Jafari, S. Chegini, and I. Turunen, "CFD simulation of mass transfer and flow behaviour around a single particle in bioleaching process," *Process Biochemistry*, vol. 44, no. 7, pp. 696–703, 2009.

[19] Y. Xu, J. Yuan, J. U. Repke, and G. Wozny, "CFD study on liquid flow behavior on inclined flat plate focusing on effect of flow rate," *Engineering Applications of Computational Fluid Mechanics*, vol. 6, no. 2, pp. 186–194, 2012.

[20] A. S. Putri, R. Amalia, T. H. Ariwibowo, and F. H. Sholihah, "Thermal characteristics of tube economizer with serrated fin," *International Electronics Symposium 2021: Wireless Technologies Intelligent Systems for Better Human Lives, IES 2021 - Proceedings*, pp. 399–404, 2021.

[21] T. Obikawa, Y. Kamata, Y. Asano, K. Nakayama, and A. W. Otieno, "Micro-liter lubrication machining of Inconel 718," *International Journal of Machine Tools & Manufacture*, vol. 48, no. 15, pp. 1605–1612, 2008.

[22] R. W. Luís, S. Carlos, and S. Paulo, "Grid convergence study of a cyclone separator using different mesh structures," vol. 55, no. 16, pp. 1–22, 2016.

[23] S. A. Chowdhury, M. N. Islam, and B. Boswell, "Temperature determination at the chip-tool interface using a computational fluid dynamics package," *International Journal of Computer Applications in Technology*, vol. 60, no. 1, pp. 27–36, 2019.

[24] T. Wu, X. Liu, W. An, Z. Huang, and H. Lyu, "A mesh optimization method using machine learning technique and variational mesh adaptation," *Chinese Journal of Aeronautics*, vol. 35, no. 3, pp. 27–41, 2022.

[25] L. N. López De Lacalle, C. Angulo, A. Lamikiz, and J. A. Sánchez, "Experimental and numerical investigation of the effect of spray cutting fluids in high speed milling," *Journal of Materials Processing Technology*, vol. 172, no. 1, pp. 11–15, 2006.

[26] E. A. Rahim, H. Dorairaju, N. Asmuin, and M. H. A. R. Mantari, "Determination of mist flow characteristic for MQL technique using Particle Image Velocimetry (PIV) and Computer Fluid Dynamics (CFD)," *Applied Mechanics and Materials*, vol. 773–774, pp. 403–407, 2015.

[27] N. Nordin, E. Benard, A. H. A. Kamal, and M. T. Ahmad, "Prediction of flow pattern behaviour behind square cylinder using computational fluid dynamic (CFD) approach," *International Journal of Integrated Engineering*, vol. 12, no. 5, pp. 137–145, 2020.

[28] C. Groth, E. Costa, and M. E. Biancolini, "RBF-based mesh morphing approach to perform icing simulations in the aviation sector," *Aircraft Engineering Aerospace Technology*, vol. 91, no. 4, pp. 620–633, 2019.

[29] N. E. Ahmad, E. Abo-Serie, and A. Gaylard, "Mesh optimization for ground vehicle Aerodynamics," *CFD Letters*, vol. 2, no. 1, pp. 54–65, 2010.

[30] M. Falcone, L. Buss, and U. Fritsching, "Model assessment of an open-source Smoothed Particle Hydrodynamics (SPH) simulation of a vibration-assisted drilling process," *Fluids*, vol. 7, no. 6, 2022.

[31] P. Jadhav and R. Deivanathan, "Numerical analysis of the effect of air pressure and oil flow rate on droplet size and tool temperature in MQL machining," in *Materials Today: Proceedings*, vol. 38, pp. 2499–2505, 2021.